PHYSICAL REVIEW B VOLUME 47, NUMBER 23 15 JUNE 1993-I

# Kinetics of crystal dissolution for a Stillinger-Weber model of silicon

Michael J. Uttormark* and Michael O. Thompson
*Department of Materials Science and Engineering, Cornell University, Ithaca, New York 14853*

Paulette Clancy[†]
*School of Chemical Engineering, Cornell University, Ithaca, New York 14853*

(Received 17 November 1992)

We present a method combining nonequilibrium molecular-dynamics simulation with Markovian data analysis techniques suitable for the study of both the growth and dissolution of crystalline "embryos" in the liquid phase. The feasibility of studying growth processes is demonstrated, but the majority of the studies concern crystal dissolution at temperatures slightly above the melting point. Molecular-dynamics simulations using the Stillinger-Weber potential were performed by embedding crystallites of 400–800 atoms in a liquid phase consisting of approximately 3600–7200 atoms, respectively. During each simulation, the time evolution of the size and shape of the embryo was followed until it became indistinguishable from the liquid. These simulations provide information on the atomic processes involved in dissolution and on the macroscopic kinetics of small clusters. The sensitivity of the results to different temperatures, system sizes, initial cluster shapes, and the criteria used to distinguish between solid and liquid are demonstrated.

## I. INTRODUCTION

Very little is known about the kinetics of liquid-to-solid transitions in the earliest stages of nucleation and growth (or dissolution of the crystal to a liquid). This important regime is extremely difficult to study experimentally due to the small time and size scales involved, and the inherent difficulties associated with experiments in the condensed environment. Subcritical cluster dynamics predominante only in the region near the nucleation temperature, and are most likely to be observed in the so-called "transient nucleation" regime. This regime is created when a liquid is cooled at a sufficiently high rate that the dynamic limitations of solid phase cluster growth are reached, and nonequilibrium populations of clusters are found within the supercooled liquid. The cooling rate can be made so extreme that critically sized clusters do not occur until temperatures which are lower than predicted by quasiequilibrium nucleation theory are reached.

Recent work by Stiffler, Thompson, and Peercy[1] has shown that homogeneous nucleation of a Si crystal from a supercooled melt can be quantified even at extremely high quench rates ($\simeq 10^{10}$–$10^{11}$ K s$^{-1}$). At the highest quench rates, the transient nucleation theory must be employed to fit the experimental supercoolings.[2] Their study provided the motivation for the work reported here involving molecular-dynamics computer-simulation studies of crystal growth and dissolution in a liquid phase. Molecular-dynamics (MD) simulation methods are an appropriate technique for studying these processes since the details of atomic motion are easily monitored. The direct simulation of spontaneous nucleation of a crystalline phase from the liquid using MD has proven to be feasible for simple potentials such as the soft sphere[3,4] and Lennard-Jones models[5–8] and for classical potential models for metals.[9–12] The most comprehensive simulation study of homogeneous nucleation of crystal from the melt was made by Swope and Andersen[8] for a system containing one million Lennard-Jones particles. They monitored the evolution and history of subcritical crystal embryos using a method based on Voronoi polyhedra. There was little system size dependence between 15 000-atom subsets and the parent one-million-particle runs, suggesting that the size-dependent artifacts had largely disappeared once the system contained around 15 000 particles. Although the liquid-to-solid transition was observed, analysis of the kinetics of the phase transformation was not performed.

Potential models for semiconductors, such as the Stillinger-Weber (SW) potential,[13] do not show spontaneous crystallization from the melt for long times [e.g., for a system of 5000 SW particles, nucleation was not observed for more than 1 ns of simulated time (Ref. 14)]. Such run times are close to the practical limit of current simulations. This sluggishness is also observed experimentally in semiconductors which crystallize at peak velocities much slower than those of simple metals. Given that spontaneous nucleation in a simulated silicon system is essentially impractical, we chose to study the closely related problem of the *dissolution* of crystalline embryos into the liquid phase at temperatures slightly above the melting point. The dissolution process was found to be relatively fast, allowing many simulations to be performed. This was crucial during the development of both the simulation methods and the analysis techniques necessary to extract the kinetics. The initial two-phase configuration was created by implanting a crystalline seed of SW-modeled Si into a liquid of the same material. The time evolution of this "subcritical" sized cluster was followed until the cluster had completely dissolved.[15] We shall also demonstrate in this paper that the growth of an implanted crystalline seed is feasible, albeit computation-

0163-1829/93/47(23)/15717(10)/$06.00

ally protracted.

The organization of the discussion is as follows. Section II describes the nonequilibrium molecular-dynamics simulation method used here. Section III describes the raw simulation data produced (mainly cluster size-time information). A sensitivity analysis of the results for a number of system variables is presented. Section IV describes the Markovian analysis of the transformation dynamics of small clusters within a MD framework and the ability to produce rate information. Section V summarizes our findings.

## II. SIMULATION DETAILS

In this paper we shall be implanting a seed crystal into a liquid phase in order to study crystal dissolution. Since the introduction of this seed represents a relatively large perturbation to the system, it is important to determine how details of the method used to configure the original state affected the results. A number of simulations were performed to assess the effects of system size, initial configuration (setup method and shape of seed), the criteria used to determine the size of the cluster, and the effect of temperature on the dissolution rates observed.

### A. Preparation of bulk phases

In order to produce a seed crystal for implantation into a liquid (as will be described here), equilibrated bulk phases were first prepared. An equilibrium liquid phase containing 4096, 5832, or 8000 SW Si atoms was simulated in an *NVT* (constant volume and temperature) ensemble at temperatures above the melting point for the Stillinger-Weber model of Si, using three-dimensional periodic boundary conditions to reduce edge effects. Values of 10–20 % above the melting point ($T_m = 1691$ K for a SW model of Si) were typically used. The volume of the system was chosen to lie on the zero-pressure coexistence line of solid and liquid, as determined by Broughton and Li.[16] The liquid configurations were prepared by heating a 0-K diamond cubic configuration to a high temperature ($\simeq 4200$ K) followed by cooling to the desired temperature by periodic rescaling of velocities over thousands of time steps. The liquid configurations at the final (desired) temperature were then further annealed for at least 10 000 time steps.

An equilibrium crystalline solid, superheated above the melting point, containing 4096, 5832, or 8000 SW Si atoms (initially placed on diamond cubic lattice sites) was simulated in an *NVT* simulation at the same final temperature as the liquid described above. The crystal was also chosen to have an appropriate volume on the solid-liquid coexistence curve. Simulations of bulk systems with periodic boundary conditions (i.e., surfaceless systems) typically superheat considerably; for the SW potential, Broughton and Li have shown that the superheated crystalline phase persists to at least 30% above the melting point.[16]

### B. Methods for inserting the seed crystal

Two different models were employed in order to achieve a system with a seed crystal of a SW model of Si surrounded by the bulk liquid. A primary goal was to create this heterogeneous system with as little disruption as possible to the thermodynamic properties of the whole system. As will be shown, inserting a seed crystal into a liquid phase causes short-lived transients which, while of little concern in other studies, must be minimized here because of their impact on the kinetics. The two methods we used to produce a seed crystal in a liquid phase are described below.

#### *1. Implanted seeds*

Crystallites of 400–800 atoms (roughly 10% of the system size) were extracted from the annealed solid configuration by selecting all atoms contained in either a cube or a sphere. A hole of the same size was created in the liquid by the removal of atoms, with additional atoms removed from the liquid in a boundary region around the solid crystallite until the nearest-neighbor distance between all liquid and solid atoms was $> 1.0\sigma$, where $\sigma$ is the length scale defined by the potential. The choice of this exclusion distance was found to minimize transient effects during the dissolution stage and is discussed further below. In our early simulations, 27 cubic crystallites were extracted from each equilibrated solid configuration. It was later shown that a spherical implant caused less of a transient than a cubic one. Each crystallite was taken from a unique position in the solid configuration, although individual atoms may have been shared between crystallites. The location of the corresponding hole in the liquid was also varied throughout the liquid configuration. Later, we performed a limited study to try to ascertain the minimum number of repetitions of the simulation from different starting points necessary to give acceptable statistical data about the dissolution process. We found that eight runs from different starting points was inadequate, but that 14 runs from different origins gave comparable statistics to that obtained using 27. In the later stages of our studies we used 14 different starting points to balance statistical adequacy against computing time.

#### *2. The "frozen section" method*

In this approach, the system originally consisted of a crystal equilibrated at a temperature above the melting point. The positions of atoms within a central spherical region were held fixed while the remainder of the system was heated to a temperature well above the melting point to create a liquid phase around the fixed crystal seed. The liquid portion was then cooled slowly to the desired temperature. Once the system reached equilibrium, the atoms of the central seed crystal were allowed to move. This method produced less transient effects and represents a preferable method of seed crystal insertion.

### C. Procedural Details

The simulations for the dissolution of the crystal were performed in the microcanonical ensemble where the number of particles, volume, and total energy of the system are fixed (i.e., an NVE system). As mentioned earlier, the forces between the particles were modeled using the Stillinger-Weber model.[13] A time step of 1.5 fs provided energy conservation to 1 part in $10^5$. Some simulations were performed with a time step of 0.5 fs to produce smooth motion on a videotape realization of the simulation results.

The system sizes used in these studies range from 4000–8000 atoms. System size-related effects are a recurring problem in simulations of crystal growth; not only the thermodynamic properties, but also the dynamic (transport) properties are affected if the system size is too small.[17,18] It will be shown that size effects are also evident here. Periodic boundary conditions were employed on all faces of the cubic simulation cell. Since these boundary conditions are known to enhance crystallization for small system sizes, there was a need to use as large a system size as possible. The seed crystal must be surrounded by a large quantity of liquid to avoid the unwanted interaction of the seed crystal with its periodic image in the neighboring cells. In addition, for growth studies, the presence of the periodic boundary conditions placed an upper limit on the crystal size which can be grown for a given system size. The upper limit is reached when the seed crystal (and the surrounding interfacial layers) grows sufficiently large for it to interact with its image(s). Again, this required the use of a large system size.

The simulations were performed on a Convex C210 machine. A fully vectorized FORTRAN SW MD code, optimized for this machine, produced a throughput of $3.6\times10^6$ particle-time steps per CPU hour. Graphical analysis of the resulting atomic configurations was made using the MOLPIC software package[19] on a Silicon Graphics Inc. Iris 3000 series work station and subsequently processed through a Qutron video animation system to produce a videotape of the dissolution process.

### D. Recognition criteria for crystal and liquid regions

The critical step in the analysis of the atomic configurations is the determination of which atoms belong to the central seed crystal (as opposed to the surrounding liquid). The derivative of this number with respect to time is the dissolution rate of the crystallite. Traditionally used system properties, such as order parameters, radial distribution functions, diffusion coefficients, etc., are inappropriate here since they produce an average value of the property over the entire system and are unsuitable for heterogeneous systems. Criteria that identify each individual atom as having a solidlike or liquidlike environment at a given "snapshot" in time were sought, although time-dependent (history) methods were also considered. For practical considerations, any solid-liquid selection criterion should also be mathematically and logically simple for efficient implementation. Given that the cluster size determination defines the dissolution rate, it is clearly crucial to study the effect of the criteria on the observed kinetics.

In a recent paper[20] we reported three criteria for the Stillinger-Weber model of silicon and tested their suitability for the selection of solidlike from liquidlike regions. In the "three-body" criterion, all atoms which were fourfold or fivefold coordinated (with a nearest-neighbor distance of $1.6\sigma$) and which had a three-body energy less than $0.2\epsilon$ were designated as being solid. The parameters $\sigma$ and $\epsilon$ represent the distance at which the potential energy is zero and the maximum attractive energy of the potential, respectively. A second criterion, named the Grabow criterion after its developer, is based on the coordination of the atom. In this criterion, an atom is said to be solidlike if it has four nearest neighbors and three of these atoms also have four nearest neighbors. The third criterion, the "angular" criterion, defines a solid atom as one with four nearest neighbors and a value of $A$ less than 0.4. The parameter $A$ is defined thus: Nearest neighbors around a central atom in a diamond cubic structure form size angles, all of which are 109° for the ideal lattice. If $\Theta_i$ is the value of angle $i$ and we compute the sum

$$A=\sum_{i=1}^{6}(\cos\Theta_i+\tfrac{1}{3})^2\ , \qquad (1)$$

$A$ will be zero for the ideal lattice since $\cos 109^\circ=-\frac{1}{3}$. Deviations in the angles can only increase $A$ due to the quadratic nature of the function. Since the number (and identity) of all the neighbors of a particle in a simulation are known, a cluster can be constructed by identifying all contiguous solidlike neighboring atoms. For clusters larger than 6–8 atoms, the three criteria were found to be reliable. Tests of the performance of the three criteria in distinguishing solidlike from liquidlike in a heterogeneous environment[20] showed that the Grabow criterion does not include any interfacial atoms at the solid-liquid boundary and hence provided an overly conservative measure of the size of the solid cluster. The three-body and angular criteria gave quite similar results.[20]

## III. RESULTS FOR THE CLUSTER SIZE EVOLUTION

### A. Dissolution of a seed crystal

Using the three-body criterion described above, the following results were obtained for a typical study of the dissolution of a single implanted seed crystal as a function of time for a system containing 5830 atoms. Using the seed crystal implantation method, an initial regime of rapid size decrease was always observed, followed by a period of slower dissolution (see Fig. 1). The fast dissolution regime (during the first 200 fs or so) was associated with a system equilibration period, where a new temperature and pressure were sought following the insertion of the crystallite. With the implantation method, the temperature typically rose by $\simeq 200$ K. Smaller temperature rises were observed using the "frozen section" method. A negligibly small change in pressure also occurred with the parity-violating energy consuming less than $<10^{-4}$ of the total energy. During this initial transient period, the crystallites were found to decrease in size by approximately 200 atoms. Analysis of the kinetic energy of individual atoms during this period revealed that those atoms near the liquid-solid boundary attained large kinetic ener-

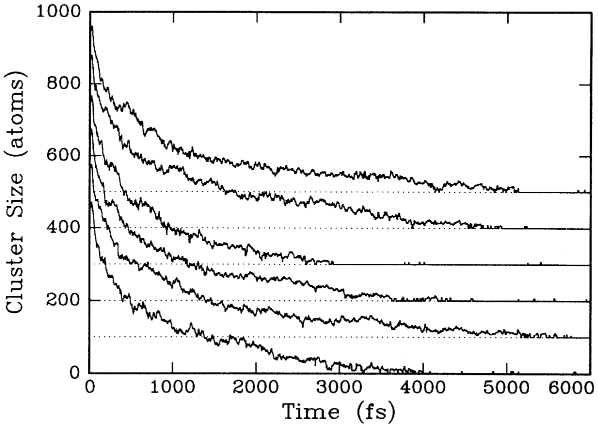

FIG. 1. Cluster size-time information for a series of simulation runs monitoring the dissolution of an implanted seed crystal into the melt. Systems of 4000 SW atoms were studied at a post-transient reduced temperature of 0.071. Note the large statistical variations between individual runs (offset for clarity). The time to dissolution, for example, varies by a factor of 2. The "average" behavior to be extracted from this data is the time for the transition from one cluster size to another.

gies but equilibrated rapidly to thermal velocities. Since the initial transient regime is caused by the perturbation of the system in response to the insertion of the crystallite, this period was excluded from the analysis which determined the dissolution rate. Cluster sizes were then followed starting from these "equilibrated" crystallites containing ≤200 atoms. Since the crystal has lost nearly one half of its original atoms at this point, the influence of the method used to construct the initial liquid-solid interface was found to be minimal.

The results of six of the 14 different seed crystals at this system size and temperature are shown in Fig. 1. Two observations are readily apparent. First, there is a considerable variation in the results for a single seed relative to the "average" behavior. Second, the size evolution of any particular crystallite is not monotonic; rather, the crystal explores many sizes (and shapes) on its path to dissolution. It is to be expected that atomic-level processes have large statistical variations between individual runs and that multiple crystallite dissolution profiles are necessary to uncover the average cluster dynamics. In order to condense the behavior of numerous individual crystallites into a representative crystallite, a statistical interpretation of the dissolution data was developed. This will be described in a subsequent section.

### B. Effects of methods used to construct the initial configuration

#### *1. Effect of the exclusion distance on cluster size*

The SW potential produces very strong repulsive forces between any pair of atoms separated by less than $1.0\sigma$. This strong repulsion is the source for the large kinetic energy seen in the interfacial region during the transient period since small interatomic spacings are a possible result of inserting the crystalline solid into the hole in the liquid. To minimize this effect, liquid atoms were removed from the interfacial region if they were found to be within a critical distance of any solid atom, termed the "exclusion distance." Studies varying this distance from $(0.8-1.2)\sigma$ showed that any value in the range $(1.0-1.2)\sigma$ produced a reasonably small transient. Using a value of $1.0\sigma$ for the exclusion distance was found to minimize the temperature increase in the "long-time" limit (representing thousands of fs). The removal of atoms is also a source of the reduction in pressure observed during the transient since the volume is held fixed and periodic boundary conditions are employed. This effect is relatively small, however, since less than 0.5% of the atoms were removed and the density difference between the solid and liquid phases is approximately 4%.

#### *2. Effect of the solid-liquid criterion on cluster size*

The result of using each of the three criteria mentioned above (and described in detail in Ref. 19) on the same set of atomic configurations is shown in Fig. 2. Since the separation of atoms into solid and liquid regions is subjective, it is not surprising that the three criteria differ in the number of atoms which are judged to be part of the solid cluster. The coordination number-based Grabow criterion is very conservative, requiring not only that there be four nearest neighbors, but also that three of these neighbors be similarly coordinated. This criterion identified the central portion of the crystalline cluster, but excluded any interfacial region. The three-body energy criterion represents the other extreme, classifying not only the same central region as solid but also some of the interfacial boundary layer between solid and liquid; the angular criterion lies in between. Due to the subjective nature of the definition, it is difficult to determine whether any criterion which produces a reasonable cluster size can be said to be more "correct" than any other. However, it is enlightening to determine the effect of the choice

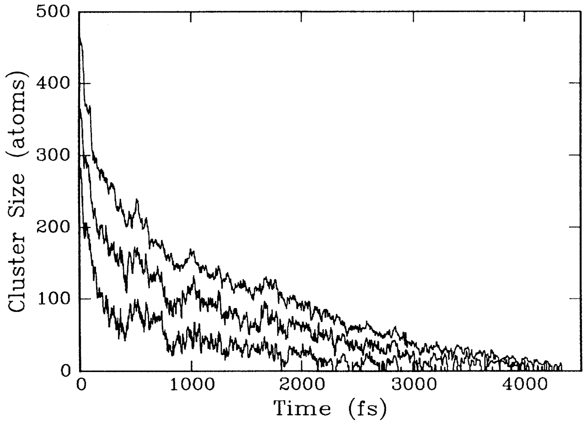

FIG. 2. The effect of criteria on the cluster size-time information. The upper curve shows the results obtained using the three-body criterion, the middle curve shows those for the angular criterion, the bottom curve shows the results for the Grabow criterion. The post-transient temperature was 0.071.

of criterion on the melting rates, as will be considered below.

### C. The effect of temperature

At temperatures below the melting point, we would expect clusters of a supercritical size to grow. However, we do not know *a priori* the critical size for a given potential model at a given undercooling. If the seed crystal proves to be subcritical, the seed crystal has a tendency to dissolve, though there is a finite probability that it may grow, depending on the detailed specifics of the local environment of the crystal. As an example of this, we prepared a system with an 800-atom seed crystal equilibrated in a liquid phase containing 7200 atoms at a reduced temperature of 0.06 (i.e., at a temperature corresponding to 85% of $T_m$). The system was prepared using the "frozen section" method described in Sec. II. The temperature was chosen to correspond to the maximum in the interface response function (i.e., the interface velocity-interface temperature relationship). The maximum velocity was found experimentally to be approximately 14 m/s at $0.85T_m$ for Si.[22] A single simulation was run at this temperature for 60 000 time steps (corresponding to 160 h of computer time) by which time the cluster had completely melted. Later evaluation of the interfacial surface tension estimated the critical cluster size for growth at this temperature to be 1400 atoms, substantially greater than the size of the implanted seed crystal.

A second seed crystal was prepared containing 600 crystalline atoms in a liquid phase containing 5200 atoms using the frozen section method. This time the reduced temperature was set at 0.04, corresponding to 60% of $T_m$. An estimate of the critical cluster size at this lower temperature is 140 atoms, thus the implanted 600-atom seed crystal should have a high probability of growing at this temperature. As shown in Fig. 3, the seed crystal grew to a size of 1600 atoms after 120 ps of simulation (i.e., 120 000 time steps), at which point the simulation was terminated. No kinetic rate information was extracted from this single-growth simulation. The purpose of its inclusion here is to show that the methods are equally applicable to crystal-growth studies as well as crystal dissolution.

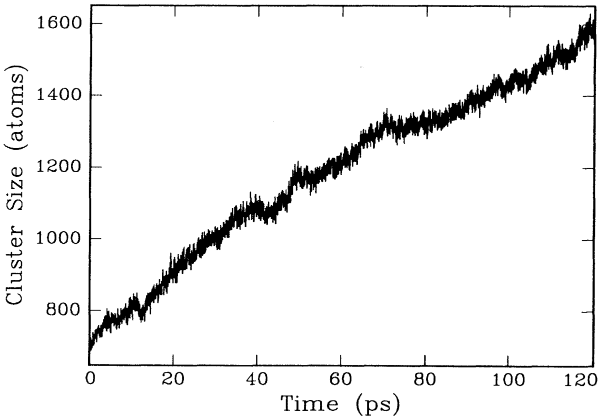

FIG. 3. Growth of an implanted crystal initially containing 600 atoms at a reduced temperature of 0.04.

One final piece of information can be extracted from the two simulations described in this section. Since one of these simulations describes growth and the other dissolution of the crystal, the two simulations provide bounds for the interfacial free energy $\gamma$ for the Stillinger-Weber potential. Given the two different undercoolings represented by the simulations described above, this leads to values of $\gamma^*$ (the reduced free energy) in the range $0.027 \leq \gamma^* \leq 0.096$ or $0.21 \leq \gamma \leq 0.75$ J m$^{-2}$, assuming a size-independent $\gamma$. Since the melting of the larger crystal was quite slow, one would expect the value of $\gamma$ to be nearer the lower end of the range. This is consistent with previous measurements by Stiffler, Thompson, and Peercy[1] for real silicon (0.34 J m$^{-2}$) and by Grabow for the SW model of Si (0.26 J m$^{-2}$).[23] Dissolution studies of crystalline clusters at two different temperatures above the melting point of a SW model of Si were performed for detailed analysis. The clusters each contained 580 atoms inserted into a liquid containing 5200 atoms. As expected, the results showed that the clusters melted more rapidly at higher temperatures. Quantitative determination of the melting rates as a function of size and temperature are discussed in the next section.

## IV. DETERMINATION OF MELTING RATES

A seen in Fig. 1(b), the dissolution process is clearly statistical with substantial variations between individual runs. Although each of the 14 "histories" shown in this figure were derived from clusters taken from the same initial solid, the time to absorption in the liquid varies by a factor of 2. Clearly, there is an underlying "average" behavior, but extraction of this dissolution rate requires more than simple curve fitting. Since information on the dissolution process is contained in every change in cluster size in each run, the behavior can be properly analyzed using the formalism of an absorbing Markov chain[24] from a transition-probability matrix. This method provides a quantitative means for determining dissolution rates as a function of cluster size and temperature.

To apply the Markov method to this melting process, maximum and minimum cluster sizes are chosen for the absorbing states; that is, cluster sizes which are considered end points and which do not evolve further with time. The lower limit is set by the size considered to be fully melted into the liquid, i.e., six atoms in this work. For large clusters, the number of transitions observed in the simulation is low and the upper limit must be set based on statistical constraints. Between these two limits, all of the simulation runs at a given temperature were analyzed to determine the probability for transitions from size $i$ to size $j$ during one time step, building up a transition-probability matrix $\Lambda$, where the number of clusters at time $i+1(\mathbf{n}_{i+1})$ is related to the number at time $i$ through

$$\mathbf{n}_{i+1} = \Lambda \mathbf{n}_i \ .$$

Although the absorbing states are included for purposes of determining the probabilities, those states are not included in $\mathbf{n}_i$ or $\Lambda$. Once this transition-probability matrix is determined, the "average time to melt" for a cluster of initial size $i$ is given by the sum of the $i$th row of the characteristic matrix $[I-\Lambda]^{-1}$.

Results for the Markov analysis from 14 clusters are shown in Fig. 4. To estimate the sensitivity of the result to the number of transitions analyzed, a second curve was determined by analyzing the dissolution of only four clusters; the resulting time to melt is shown as the dashed curve in Fig. 4. The statistical analysis of only four cluster melting dynamics was essentially identical, confirming that sufficient statistics could be obtained in only a few simulations.

A key assumption in the Markov method is that the size changes seen in the simulations are random from one time step to another, i.e., they are uncorrelated. The molecular-dynamics simulation method is completely deterministic, thus a test of the correlation length in the MD simulations was undertaken. To perform this test, the Markov chain analysis was performed on the data set after every second point was eliminated and it was found the average melt times did not alter significantly. This was also true even if two of every three points were discarded. In other words, Markov transition matrices were produced by following size changes at every time step, at every second time step, and every third time step. The resulting dissolution rates were virtually identical for all three cases. Consequently, either the transitions are random at the one-time-step level or the correlation length exceeds three time steps. Given the appearance of the simulation data, we believe that the transitions are random, thus verifying the Markov assumption. Tests of longer correlation times were not possible due to the increased uncertainty in the derived rates arising from statistical fluctuations.

The mean time to dissolution is essentially an integral over the dissolution rates. Thus, rate information can be extracted from the melting time data by differentiating with respect to cluster size. This gives the average time spent at any cluster size and is the multiplicative inverse of the melting rate $dn/dt$. If $T(n)$ is the average melting time for a cluster of size $n$, then

$$\frac{dn}{dt}=\frac{-1}{dT/dn}\ , \tag{2}$$

where the minus sign has been added to preserve the convention that negative values correspond to melting. To avoid "noisy" results for the melting rate, the absorption times were fitted to a fourth-order polynomial using a least-squares technique prior to differentiation and inversion. However, there is no *a priori* reason to require the melting rates to be smooth functions of the cluster size. Indeed, the idea of "magic numbers" (i.e., sizes that are particularly stable) is well accepted for clusters in the vapor phase. However, there were no obvious discontinuities in the data and the smoothing procedure permitted comparison of the results with predictions of classical nucleation theory[25] which has no provision for magic numbers.

There are several parameters that must be arbitrarily chosen when using this Markov method to reduce the transition data to a melting rate. These are the largest size cluster included in the Markov chain, the smallest size, and the order of the polynomial used to fit the melting times. Variation in the minimum size shifts the zero in the average melting time but otherwise leaves the shape of the melting curve largely unchanged. This shift is subsequently lost in the differentiation step and hence does not affect the melting rates. Figure 5 shows the calculated melting rate for upper limit sizes of 200, 300, and 400 atoms. Variation in the largest cluster size affected the melting rates only in the region closest to the maximum size ($\simeq 175$ atoms for the 200-atom case). Several factors contribute to this behavior. First, large clusters appear closer to the initial transient period in the simula-

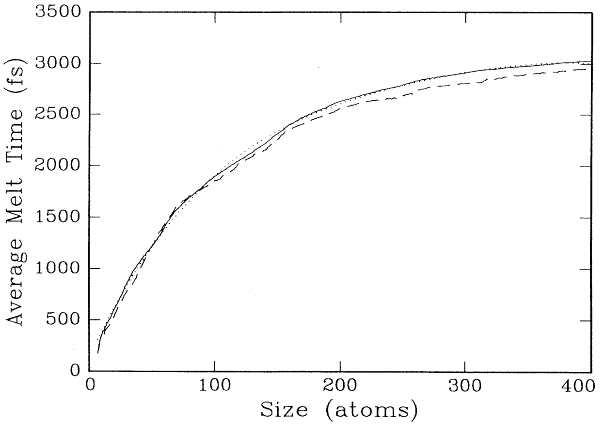

FIG. 4. The average time to melt calculated from an analysis of 14 clusters (solid line) and for four clusters (dashed line). Although the "noise" increases for the four-cluster set, the average behavior is unchanged. The dotted line is a fourth-order polynomial fit to the solid curve.

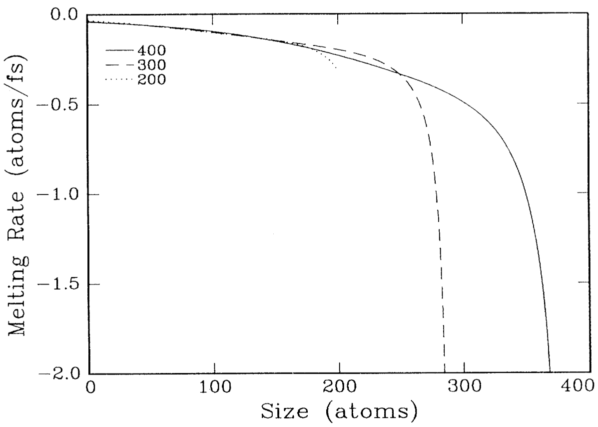

FIG. 5. Effect of the maximum cluster size choice (400, 300, 200 atoms) on the calculated melting rates as a function of size. For small clusters, the choice of the upper absorbing state is irrelevant.

tion and thus have artificially high melting rates. It was previously noted that the transient period extended approximately 500 fs into the simulation; at this time, most of the clusters were reduced to a size of about 200 atoms. Second, the polynomial fitting procedure produces a very flat function at large cluster sizes. Differentiation and inversion of this type of function is numerically unstable and can result in unphysical values. The flatness of the absorption-time profile at large sizes is also a result of the finite size of the transition matrix. At intermediate sizes, most transitions which increase and decrease the size of the cluster are included in the construction of the transition-probability matrix. At the larger extreme, most of the "increasing" transitions are not counted since they produce clusters larger than the maximum size allowed.

### A. Effect of solid-liquid criterion

Different melting rates were produced by the three criteria (three-body, Grabow, and angular criteria) investigated. Figure 6 shows the melting rates produced from a set of 14 clusters of original size $\simeq 570$ atoms in a liquid of 5200 atoms at a post-transient temperature of 0.081. In each case, the maximum size was chosen as the size at time 500 fs. This corresponded to 80 atoms for the Grabow criterion, 150 for the angular criterion, and 200 atoms for the three-body energy criterion. However, since the three criteria produce different cluster sizes for a given configuration, the melting rates are not expected to agree. It is more reasonable to compare the relative melting rates $(1/n)dn/dt$ as shown in Fig. 7. This showed that the results for the three-body and angular criteria are very similar, whereas the Grabow criterion gives quite different values. This result again reflects the overly conservative size estimate of the Grabow criterion.

Another possible scaling relationship to compare the results from the three criteria can be derived by considering the "thickness" of the interfacial boundary layer produced by each criterion. Let $N_G$ be the number of atoms that the Grabow criterion identifies as solid for a given configuration. Then the number of atoms identified by the angular criterion is

$$N_A = \frac{4\pi}{3}\left[\left[\frac{3N_G}{4\pi}\right]^{1/3} - r_G^A\right]^3 , \tag{3}$$

assuming that the two criteria differ only in their inclusion or exclusion of an interfacial region whose (constant) thickness is $r_G^A$. Figure 8 shows the melting rates for the original three-body criterion compared to those for the transformed angular and Grabow criteria data. Values of $r$ of 0.5 and 1.4, respectively, represented the best fit to the data. In this case, quite good agreement was found for the three criteria for a limited range of sizes.

Since the rates determined by one criterion can be related to those of the others by a reasonable mapping function, there is little advantage in using one over the other. The three-body criterion was chosen for most of

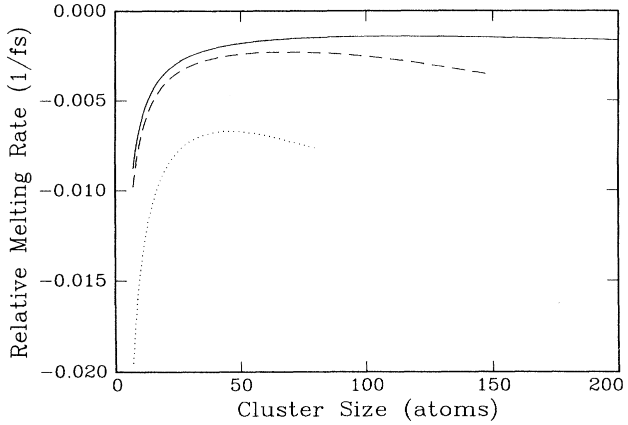

FIG. 7. Comparison of the relative melting rates for the three criteria. Key as for Fig. 6.

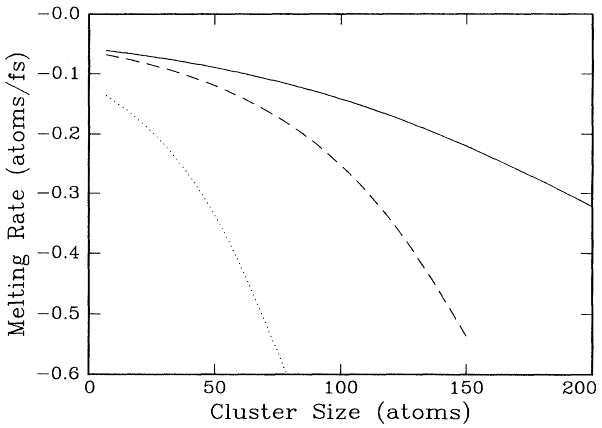

FIG. 6. Effect of the criterion on the melting rates obtained from a set of 14 clusters (for each criterion) at a temperature of 0.081. Results for the three-body criterion are shown as a solid line, those for the angular criterion by a dashed line and those for the Grabow criterion by a dotted line.

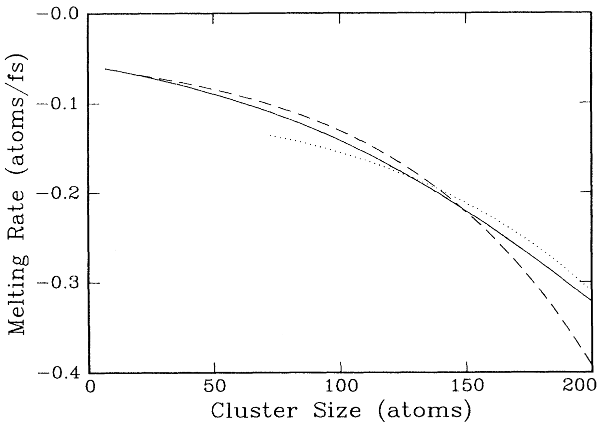

FIG. 8. Comparison of the melting rate obtained using the original three-body criterion with those for the "transformed" angular and Grabow criteria. Key as for Fig. 6.

the studies since it was easier to compute than the angular criterion, and was more stable to changes in parameters than the Grabow criterion.

### B. Effect of initial crystal size

If the melting of the cluster is a random process, then clusters of the same size should melt at the same rate, independent of their original size. Figure 9 shows the melting rates of three implanted clusters whose starting sizes were 400, 570, and 800 atoms. The observed temperature and pressure in each case was the same within normal fluctuations. It was seen that larger clusters melt more slowly, although the difference between the clusters of size 400 and 570 is much larger than that between 570 and 800. The differences in the melting rates are ascribed to system size effects. The 400-, 570-, and 800-atom clusters were inserted into liquids of 3600, 5260, and 7200 atoms, respectively. Thus, when the 800-atom implant is reduced by melting to a size of 200 atoms it is surrounded by a liquid phase containing 7800 atoms, whereas the liquid phase for the initially 400-atom cluster contained only 3800 atoms at that point. If these volumes are not large enough to behave as infinite liquids, the dynamics of the system will be affected. It is also possible that long-lived transient effects are also still present in the systems. The larger clusters require more time to melt, permitting more relaxation to occur before reaching the smaller sizes. The rates appear to be converging, however, suggesting that the size effects are diminishing. Studies of systems containing more than 8000 atoms were not performed due to the large computation time required. However, the size dependence only affects the quantitative rates and all simulations show essentially identical qualitative behavior. This qualitative behavior will be discussed further in a subsequent publication.[21]

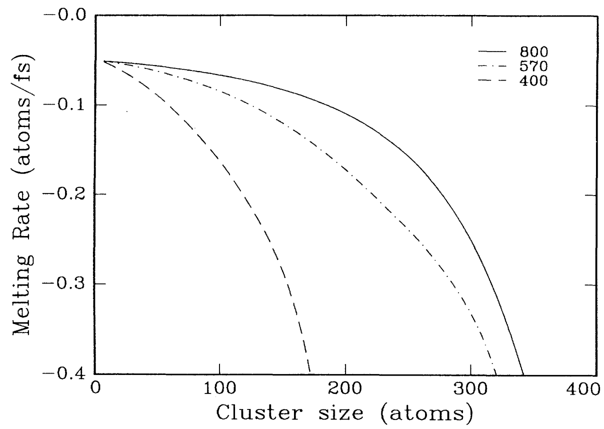

FIG. 9. Effect of system size on the melting rates. Results are shown for implanted crystalline seed crystals containing 800 (solid line), 570 (dot-dashed line), and 400 atoms (dashed line).

### C. Effect of temperature

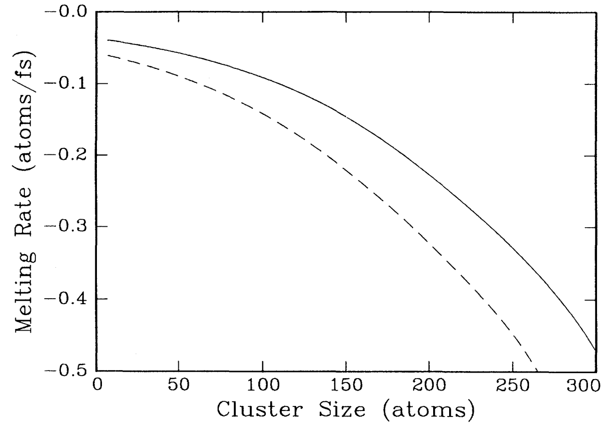

FIG. 10. Effect of temperature on the melting rates. Results are shown for two temperatures, 0.071 (solid line) and 0.081 (dashed line).

The melting rates for two sets of clusters starting with a size of $\simeq 570$ atoms are shown in Fig. 10. The post-transient temperatures for the two sets of simulations are 0.071 and 0.081. As expected, the higher temperature produced higher melting rates. Thermal activation is expected to control the melting rate and hence the rates should have a temperature dependence of the form

$$R = R_0(n)\exp\left[-\frac{E_a}{k_B T}\right], \tag{4}$$

where $R_0$ is a function of the size of the cluster. At any given size $n$, the value of the activation energy $E_a$ can be determined from the two rates $R_1$ and $R_2$ and the corresponding temperatures $T_1$ and $T_2$.

This activation energy as a function of cluster size is shown in Fig. 11. The activation energy remains in the range $(0.20-0.25)\epsilon$ for a large fraction of the clusters under consideration; larger sizes may be affected by transient effects and thus show larger statistical variation.

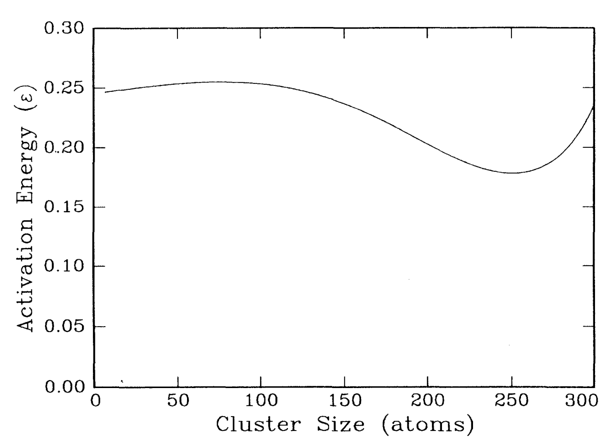

FIG. 11. The apparent activation energy as a function of size for the dissolution of crystalline clusters.

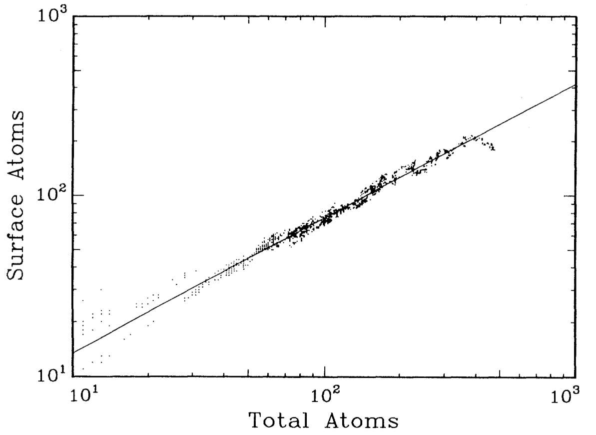

FIG. 12. The number of surface atoms in the cluster as a function of the total number of atoms comprising the cluster. The line represents a straight-line fit to the data with a slope of 0.75.

### D. Cluster shapes

Classical nucleation theory assumes the shape of the cluster to be self-similar (cubes, spheres, etc.) for all sizes. This assumption enters into the rate equations in two places. First, the driving force for melting incorporates a term proportional to the surface area of the cluster, resulting in a term containing $n^{(2/3-1)}=n^{-1/3}$. Second, the kinetic terms introduce a factor of $n^{2/3}$ into the prefactor which relates the number of attachment-detachment sites to the cluster size. When a model of the diamond cubic structure with $\leq 100$ atoms and a roughly spherical shape is examined, one finds very few atoms which could be unambiguously said to possess bulklike characteristics. Most of the atoms have at least one unsatisfied tetrahedral bond, implying that these atoms are part of the interface. Thus it is appropriate to ask whether the $n^{2/3}$ dependence of the surface area on the cluster size is applicable at these small sizes.

A scheme was devised to test the $n^{2/3}$ dependence of the surface area by defining surface atoms as any solid atom with one or more liquid atoms as nearest neighbors. The number of surface atoms as a function of the entire cluster size is shown in Fig. 12 using the three-body energy criterion to distinguish solidlike from liquidlike atoms. The slope of the line shown in the figure is 0.75, not $\frac{2}{3}$ as predicted above. The same analysis using the Grabow and angular criteria produces slopes of 0.83 and 0.75, respectively. These results would suggest that the $n^{2/3}$ dependence may not be appropriate to describe the early stages of growth in tetrahedrally bonded systems.

## V. SUMMARY

A molecular-dynamics technique for studying the dynamics of crystal clusters in a liquid matrix has been developed. A Markov chain method was used to determine the melting rates from the cluster size data. The method was shown to have excellent stability for the determination of post-transient melting rates. Three solid-liquid criteria were examined in this context. The three methods produced similar melting characteristics, but differed in the absolute value of the melting rates.

The simulation of melting and growth for a pair of clusters at a temperature below the melting point was used to place bounds on the interfacial free energy. The range obtained is consistent with previous experimental and simulation results. Comparison of melting rates for clusters at different temperatures above $T_m$ support a thermally activated process with no apparent activation energy at $(0.22-0.25)\epsilon$. At small sizes, the surface area of the clusters is proportional to $n^{3/4}$. This suggests that nearly all atoms in a small cluster are affected by the presence of the solid-liquid interface.

Although some size-dependent effects were observed in this work, the qualitative behavior is insensitive. Consequently, MD simulations of cluster growth and dissolution allow critical tests of nonequilibrium transient nucleation theory to be performed.

## ACKNOWLEDGMENTS

This work was supported by the National Science Foundation (Grant No. DMR89-3333). The authors are also grateful to the Cornell Materials Science Center for providing computing time on the Convex machine.

---

[*] Present address: Department of Materials Science and Engineering, University of Wisconsin–Madison, Madison, WI 53706.

[†] Author to whom correspondence should be addressed.

[1] S. R. Stiffler, M. O. Thompson, and P. S. Peercy, Phys. Rev. Lett. **60**, 2519 (1988).

[2] P. V. Evans and S. R. Stiffler, Acta. Metall. **39**, 2727 (1991).

[3] M. Tanemura, Y. Hiwatari, H. Matsuda, T. Ogawa, N. Ogita, and A. Ueda, Prog. Theor. Phys. **58**, 1079 (1977).

[4] M. Tanemura, Y. Hiwatari, H. Matsuda, T. Ogawa, N. Ogita, and A. Ueda, Prog. Theor. Phys. **59**, 323 (1978).

[5] M. J. Mandell, J. P. McTague, and A. Rahman, J. Chem. Phys. **64**, 3699 (1976); **66**, 3070 (1977).

[6] R. D. Mountain and A. C. Brown, J. Chem. Phys. Chem. **80**, 2703 (1984).

[7] J. D. Honeycutt and H. C. Andersen, J. Phys. Chem. **90**, 1585 (1986).

[8] W. C. Swope and H. C. Andersen, Phys. Rev. B **41**, 7042 (1990).

[9] C. S. Hsu and A. Rahman, J. Chem. Phys. **70**, 5234 (1979).

[10] C. S. Hsu and A. Rahman, J. Chem. Phys. **71**, 4974 (1979).

[11] A. Rahman, Phys. Rev. A **9**, 1667 (1974).

[12] K. Tsumuraya, M. S. Watanabe, and S. K. Ikeda, Trans. Iron Steel Inst. Jpn. **28**, 869 (1988).

[13] F. H. Stillinger and T. A. Weber, Phys. Rev. B **31**, 5262 (1985).

[14] M. H. Grabow (unpublished).

[15] All clusters are metastable (i.e., subcritical) at temperatures above the melting point and will dissolve into the melt given sufficient time.

[16] J. Q. Broughton and X. P. Li, Phys. Rev. B **35**, 9120 (1987).

[17] E. Burke, J. Q. Broughton, and G. H. Gilmer, J. Phys. Chem. **89**, 1030 (1988).

[18] D. K. Chokappa, S. J. Cook, and P. Clancy, Phys. Rev. B **39**, 10 075 (1989).

[19] MOLPIC is a three-dimensional visualization package for molecular modeling written by Dr. S. M. Thompson at Cornell University.

[20] M. J. Uttormark, M. O. Thompson, L. A. Baez, and P. Clancy, Mol. Sim. (to be published).

[21] M. J. Uttormark, P. Clancy, and M. O. Thompson (unpublished).

[22] J. Y. Tsao, M. J. Aziz, Michael O. Thompson, and P. S. Peercy, Phys. Rev. Lett. **56**, 2712 (1986).

[23] M. H. Grabow (private communication).

[24] J. G. Kemeny and J. L. Snell, *Finite Markov Chains* (Van Nostrand, Princeton, NJ, 1960).

[25] For example, K. F. Kelton and A. L. Greer, J. Non-Cryst. Solids **79**, 295 (1986).